

# 실제 구조계의 유한요소법에 기초한 지진 신뢰성해석

## FEM-based Seismic Reliability Analysis of Real Structural Systems

허 정 원†

Huh, Jungwon

(논문접수일 : 2005년 9월 22일 ; 심사종료일 : 2006년 6월 13일)

Haldar, Achintya\*

Haldar, Achintya

### 요 지

응답면기법, 유한요소법, 일차신뢰도법 그리고 반복 선형보간기법을 합리적으로 결합한 정교한 신뢰성해석 기법이 지진하중을 포함하는 단기 동적하중을 받는 복잡한 실제 비선형 동적구조계의 신뢰성 평가를 위하여 제안되었다. 기법은 하중 및 저항과 관련된 랜덤변수의 비선형성과 불확실성의 모든 중요 원천을 명시적으로 고려한다. 본 기법의 특징은 전통적 랜덤진동방법의 대안으로서 지진하중을 시간영역에서 적용하는 것이다. 실제 강프레임의 연결부에 대한 유연성을 표현하기 위하여 4-매개변수 리차드 모델을 사용하였다. 리차드 매개변수의 불확실성에 대한 고려도 알고리즘에 포함하였다. 다음으로 횡방향으로 유연한 강프레임을 철근콘크리트 전단벽으로 보강하였다. 균열 발생 후 전단벽에서의 강도저감 또한 고려되었다. 강철 연결부를 갖는 횡방향으로 유연한 강프레임, 각기 다른 강성의 부분강철 연결부를 갖는 강프레임, 그리고 콘크리트 전단벽으로 보강된 강프레임의 세 구조물을 고려함으로써 실제 구조물의 신뢰성평가를 위한 기법의 적용성을 검증하였다.

**핵심용어** : 유한요소법, 지진신뢰성평가, 부분강철 연결부, 응답면, 한계상태, 전단벽, 불확실성

### Abstract

A sophisticated reliability analysis method is proposed to evaluate the reliability of real nonlinear complicated dynamic structural systems excited by short duration dynamic loadings like earthquake motions by intelligently integrating the response surface method, the finite element method, the first-order reliability method, and the iterative linear interpolation scheme. The method explicitly considers all major sources of nonlinearity and uncertainty in the load and resistance-related random variables. The unique feature of the technique is that the seismic loading is applied in the time domain, providing an alternative to the classical random vibration approach. The four-parameter Richard model is used to represent the flexibility of connections of real steel frames. Uncertainties in the Richard parameters are also incorporated in the algorithm. The laterally flexible steel frame is then reinforced with reinforced concrete shear walls. The stiffness degradation of shear walls after cracking is also considered. The applicability of the method to estimate the reliability of real structures is demonstrated by considering three examples; a laterally flexible steel frame with fully restrained connections, the same steel frame with partially restrained connections with different rigidities, and a steel frame reinforced with concrete shear walls.

**Keywords** : finite element method, seismic reliability assessment, PR connection, response surface, limit state, shear wall, uncertainty

## 1. INTRODUCTION

Despite significant recent progresses in the risk and reliability analysis techniques, a large segment of the engineering profession appears to be un-

familiar with them and thus fails to use them in everyday practice. Some of the major factors are that they are not similar or parallel to the deterministic methods used in analyzing real structures and they cannot capture the realistic struc-

† 책임저자, 정회원 · 전남대학교 해양기술학부 해양공학전공 조교수  
전화: 061-659-3153 ; Fax: 061-659-3150  
E-mail: jwonhuh@chonnam.ac.kr

\* Professor, The University of Arizona, Tucson, AZ85721, U.S.A., haldar@u.arizona.edu

• 이 논문에 대한 토론을 2006년 9월 30일까지 본 학회에 보내주시면 2006년 12월호에 그 결과를 게재하겠습니다.

tural behavior. It is expected that once the applicability of probabilistic methods in estimating the reliability of real complex structures is successfully demonstrated, the reliability-based design and analysis concepts will be used more widely by the deterministic community. In developing such a method for the reliability evaluation of real structural systems, it is necessary to first use improved deterministic algorithm by incorporating the realistic structural behavior using advanced computational power. Then, it is necessary to extend the deterministic algorithm to include the uncertainty in the problem, producing a new reliability estimation procedure.

The estimation of the probability of failure implies that structural behavior just before failure needs to be captured as accurately as possible. Major sources of nonlinearity including geometric and material, boundary or support, and connection conditions, must be modeled realistically. The most rigorous deterministic dynamic analysis requires that the loading must be applied in time domain. Thus, the reliability analyses of dynamic structural systems also need to be conducted under similar conditions.

The finite element method (FEM) is commonly used to study the behavior of real structures under static and dynamic loadings assuming all the load and resistance-related variables are known or deterministic. For the reliability community, the use of advanced FEM adds two different challenges. The first challenge is how to improve the computational efficiency of the deterministic algorithm. If standard procedures are followed, the probabilistic algorithm could be inefficient or impractical. The second challenge is how to incorporate uncertainty into the improved deterministic algorithm. In the most sophisticated deterministic dynamic response evaluation procedure, the dynamic loading including the seismic loading is applied in the time domain. However, the time history of a future earthquake is unknown, and this introduces a major source of uncertainty. The representation of a dynamic load

in the form of the power spectral density function may not be appropriate, particularly for highly nonlinear structures. Most members of the deterministic community are unaware of the intricacies of the approach. Furthermore, the nonlinearities and uncertainties in the structural parameters may need to be represented approximately. The authors recently developed a very efficient dynamic reliability analysis algorithm in time domain to comprehensively address the problem. The method is discussed in the following sections. The application potentials of the method are demonstrated with the help of several examples. The reliability of a simple steel frame under seismic loading is first evaluated by making conventional or standard assumptions, i.e., the connections are fully restrained (FR) and the frame may develop geometric and material nonlinearities. All connections are essentially partially restrained (PR) with different rigidities. Thus, in the next example, the reliability of the same frame is estimated by assuming all the connections are PR-type, adding a major source of nonlinearity and uncertainty. Ordinary steel frame can be laterally very flexible. To increase its lateral resistance during seismic excitation, reinforced concrete (RC) shear walls are generally added. It produces a dual system consisting of a flexible steel frame in-filled with RC shear walls. The reliability of such a dual system is also evaluated. These examples will clearly demonstrate the application potential of the proposed method to estimate the reliability of realistic nonlinear complicated structural system in time domain considering all major sources of nonlinearity and uncertainty.

## 2. STEEL FRAMES WITH PR CONNECTIONS AND RC SHEAR WALLS

The presence of PR connections and RC shear walls in a steel frame need to be incorporated in the deterministic FEM representation. They are briefly discussed next.

### 2.1 Modeling of PR connections

PR connections not only add a major source of nonlinearity but also they dissipate energy at a much higher level. The commonly used analytical procedures developed for FR connections cannot be used to represent PR connections. The PR connections change the dynamic properties, such as the natural frequency, stiffness, damping, etc. of structures, and add a major source of uncertainty in the reliability analysis during loading, unloading, and reloading stages of dynamic excitation. The behavior of a steel frame will thus depend on how the PR connections are modeled in any nonlinear algorithm (Huh & Haldar, 2002).

Generally a relationship between the moment  $M$ , transmitted by the connection, and the relative rotation angle  $\theta$  is utilized to represent the flexibility in the connections. Although several alternatives (piecewise linear model, polynomial model, exponential model, B-Spline model, etc.) are available to represent moment-rotation behavior of connections in the literature (Haldar & Mahadevan, 2000), the Richard four-parameter model (Richard & Abbott, 1975) is chosen here. It has many advantages (Richard & Abbott, 1975; Huh & Cho, 2001). The loading, unloading, and re-loading behavior of a typical PR connection is shown in Fig. 1. The relationship, i.e.  $M$ - $\theta$  curve can be mathematically expressed as:

$$M = \frac{(k - k_p)\theta}{\left(1 + \left|\frac{(k - k_p)\theta}{M_0}\right|^N\right)^{1/N}} + k_p\theta \quad (1)$$

where  $M$  is the moment,  $\theta$  is the relative rotation between the connecting elements,  $k$  is the initial stiffness,  $k_p$  is the plastic stiffness,  $M_0$  is the reference moment, and  $N$  is the curve shape parameter.

Equation (1) represents only the monotonically increasing loading portion of the  $M$ - $\theta$  curves.

Colson (1991) and El-Salti (1992) theoretically developed the unloading and reloading parts of the  $M$ - $\theta$  curves using the Masing rule. The unloading and reloading relationships of a PR connection used in this study can be represented as:

$$M = M_a - \frac{(k - k_p)(\theta_a - \theta)}{\left(1 + \left|\frac{(k - k_p)(\theta_a - \theta)}{2M_0}\right|^N\right)^{1/N}} - k_p(\theta_a - \theta) \quad (2)$$

If  $(M_b, \theta_b)$  is the next load reversal point, the reloading relationship between  $M$  and  $\theta$  can be obtained by simply replacing  $(M_a, \theta_a)$  with  $(M_b, \theta_b)$  in Eq. (2). Therefore, the proposed method uses Eq. (1) when the connection is loading and Eq. (2) when the connection is unloading and reloading. This represents hysteretic behavior of the PR connections as shown in Fig. 1.

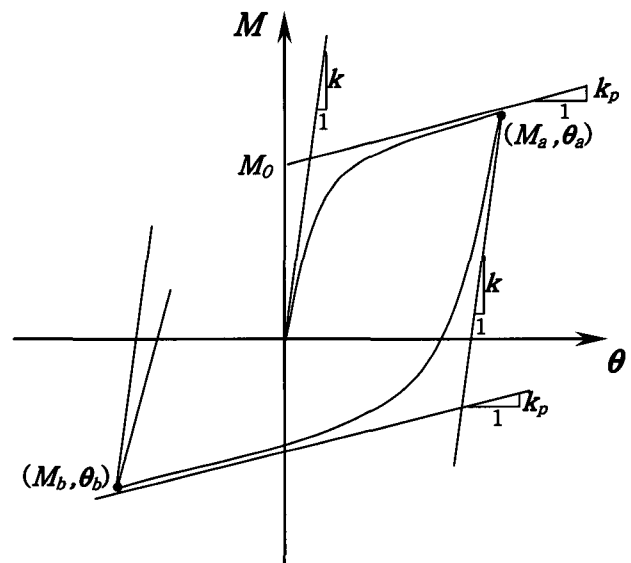


Figure 1 Loading, unloading, and reverse loading model of PR connections

### 2.2 Modeling of RC shear walls

As mentioned earlier, ordinary steel frames in the presence of PR connections may not be able to transfer horizontal loads (e.g. wind and earthquake) effectively. To improve the lateral strength of steel frames shear walls are very commonly

used. RC shear walls are considered in this study. Members of steel frames are generally represented by beam-column elements (Huh & Haldar, 2002). Representing RC shear walls by finite elements is an open question. To maintain simplicity in the proposed method, they are represented by plane stress elements. The two FEM representations need to be combined, however, the task is expected to be challenging. Moreover, the uncertainty associated with all the variables in such representations should be incorporated as accurately as possible.

In this study, the basic frame is modeled by two-dimensional (2-D) beam-column elements and the shear walls are modeled by 4-node plane stress elements. The shape of the shear wall is restricted to be rectangular. Two displacement (horizontal and vertical) dynamic degrees of freedom (DDOFs) are used at each node point. The rotation of the combined system at the node point is assumed to be very small and was independently verified using a commercially available computer program. In order to bring the shear wall stiffness into the frame structure, the stiffness of the shear walls is added to the corresponding element of the frame stiffness. The stiffness matrix of a 4-node plane stress element can be expressed as (Lee, 2000):

$$\mathbf{K}_{sh} = \frac{t}{4\gamma} \mathbf{A}'\mathbf{E}\mathbf{A} + \frac{t}{12\gamma} \mathbf{B}'\mathbf{E}\mathbf{B} + \frac{t\gamma}{12} \mathbf{C}'\mathbf{E}\mathbf{C} \quad (3)$$

where  $t$  is thickness of the wall,  $\gamma$  is the ratio of  $b$  and  $a$ ; i.e.,  $\gamma = b/a$ ,  $2a$  and  $2b$  are long and short dimensions of the rectangular shear wall, respectively. The matrixes  $\mathbf{A}$ ,  $\mathbf{B}$ ,  $\mathbf{C}$ , and  $\mathbf{E}$  in Eq. (3) can be expressed as:

$$\mathbf{A} = \begin{bmatrix} -\gamma & 0 & \gamma & 0 & \gamma & 0 & -\gamma & 0 \\ 0 & -1 & 0 & -1 & 0 & 1 & 0 & 1 \\ -1 & -\gamma & -1 & \gamma & 1 & \gamma & 1 & -\gamma \end{bmatrix} \quad (4)$$

$$\mathbf{B} = \begin{bmatrix} 0 & 0 & 0 & 0 & 0 & 0 & 0 & 0 \\ 0 & 1 & 0 & -1 & 0 & 1 & 0 & -1 \\ 1 & 0 & -1 & 0 & 1 & 0 & -1 & 0 \end{bmatrix} \quad (5)$$

$$\mathbf{C} = \begin{bmatrix} 1 & 0 & -1 & 0 & 1 & 0 & -1 & 0 \\ 0 & 0 & 0 & 0 & 0 & 0 & 0 & 0 \\ 0 & 1 & 0 & -1 & 0 & 1 & 0 & -1 \end{bmatrix} \quad (6)$$

$$\text{and } \mathbf{E} = \frac{E_c}{1-\nu^2} \begin{bmatrix} 1 & \nu & 0 \\ \nu & 1 & 0 \\ 0 & 0 & \frac{1-\nu}{2} \end{bmatrix} \quad (7)$$

where  $E_c$  is modulus of elasticity and  $\nu$  is Poisson's ratio of shear walls.

For the RC shear walls, two additional parameters, namely, the modulus of elasticity and the Poisson ratio of concrete, are necessary in the deterministic formulation as can be seen in Eq. (7). The effect of cracking in RC shear walls is another challenge that needs to be addressed in the proposed algorithm. There has been extensive research on cracking in RC panels (Gupta & Akbar, 1983 Liauw & Kwan, 1985 Vecchio, 1989 Lefas et al., 1990 Inoue et al., 1997). It has been observed that the degradation of the stiffness of the shear walls occurs after cracking and can be considered effectively by reducing the modulus of elasticity of the shear walls. Lefas et al. (1990) reported that the degradation of the stiffness after cracking could vary from 40% to 70% of the original stiffness depending on the amount of reinforcement and the intensity of axial loads. The same concept is used in this study. The shear wall is assumed to develop cracks when the tensile stress in concrete exceeds the prescribed value. The rupture strength of concrete,  $f_r$ , is assumed to be  $f_r = 7.5 \times \sqrt{f_c'}$ , where  $f_c'$  is the compressive strength of concrete.

### 3. A FEM-BASED HYBRID TIME-DOMAIN RELIABILITY METHOD

The proposed FEM-based hybrid method attempts to address issues associated with the reliability estimation when the limit state functions are implicit. The explicit limit state function of a real frame structure under short duration dynamic load-

ings is generated using the concepts of the re-sponse surface method (RSM) and FEM approach. An iterative linear interpolation scheme and the first-order reliability method (FORM) are applied to efficiently locate the failure region. The FORM is also used to estimate the risk associated with the problem under consideration. The integration of these logics forms the foundation of the proposed hybrid approach. Some of their essential features of the method are further explained next.

### 3.1 Deterministic FEM formulation

FEM-based algorithms are routinely used to represent nonlinear steel frames with FR and PR connections. However, the commonly-used displacement-based FEM may not be efficient for the reliability evaluation. To increase the efficiency in the numerical algorithm to study highly nonlinear behavior, the assumed stress-based dynamic FEM (Kondoh & Atluri, 1987 Shi & Atluri, 1988 Haldar & Nee, 1989) can be used and is used in this study. In this approach, the tangent stiffness can be expressed in an explicit form without performing any integration and fewer elements are required to describe a large deformation configuration. It is shown to be very accurate and efficient in analyzing nonlinear responses of frames (Shi & Atluri, 1988 Haldar & Gao, 1997).

The nonlinear dynamic equilibrium equation can be expressed at time  $t+\Delta t$  as:

$$\mathbf{M} {}^{t+\Delta t}\ddot{\mathbf{D}}^{(n)} + {}^t\mathbf{C} {}^{t+\Delta t}\dot{\mathbf{D}}^{(n)} + {}^t\mathbf{K}^{(n)} {}^{t+\Delta t}\Delta\mathbf{D}^{(n)} = {}^{t+\Delta t}\mathbf{F}^{(n)} - {}^{t+\Delta t}\mathbf{R}^{(n-1)} - \mathbf{M} {}^{t+\Delta t}\ddot{\mathbf{D}}_g^{(n)} \quad (8)$$

where  $\mathbf{M}$  is the mass matrix,  ${}^t\mathbf{C}$  is the viscous damping coefficient matrix at time  $t$ ,  ${}^t\mathbf{K}^{(n)}$  is the global tangent stiffness matrix of the  $n^{\text{th}}$  iteration at time  $t$ ,  ${}^{t+\Delta t}\Delta\mathbf{D}^{(n)}$  is the incremental displacement vector of the  $n^{\text{th}}$  iteration at time  $t+\Delta t$ ,  ${}^{t+\Delta t}\mathbf{F}^{(n)}$  is the external load vector of the  $n^{\text{th}}$  iteration at time  $t+\Delta t$ ,  ${}^{t+\Delta t}\mathbf{R}^{(n-1)}$  is the internal force vector of the  $(n-1)^{\text{th}}$  iteration at time  $t+\Delta t$ , and  ${}^{t+\Delta t}\ddot{\mathbf{D}}_g^{(n)}$  is the

seismic ground acceleration vector of the  $n^{\text{th}}$  iteration at time  $t+\Delta t$ .

The damping matrix  ${}^t\mathbf{C}$  in Eq. (8) is considered to be viscous in this study. In a realistic seismic analysis of steel frames, the amount of damping energy to be generated will depend on the non-yielding and yielding state of the material, and the hysteretic behavior if the material yields. For mathematical simplicity, the effect of non-yielding energy dissipation is generally represented by equivalent viscous damping varying between 0.1% and 7% of the critical damping (Leger & Dussault, 1992). Among many alternatives, Rayleigh-type damping is utilized to represent viscous damping in this study. It can be represented as:

$${}^t\mathbf{C} = \alpha\mathbf{M} + \gamma{}^t\mathbf{K} \quad (9)$$

where  ${}^t\mathbf{K}$  is the tangent stiffness matrix, and  $\alpha$  and  $\gamma$  are proportional constants which can be evaluated from the natural frequencies of the structure (Clough & Penzien, 1993).

#### 3.1.1 Incorporation of PR connections into the FEM

The assumed stress-based FEM approach used in this study uses a beam-column element to model both regular structural elements and flexible connections. However, the stiffness of PR connections needs to be updated at every iteration since it depends on  $\theta$ . This can be accomplished by updating the Young's modulus as:

$$E_c(\theta) = \frac{l_c}{I_c} K_c(\theta) = \frac{l_c}{I_c} \frac{\partial M(\theta)}{\partial \theta} \quad (10)$$

where  $l_c$ ,  $I_c$ , and  $K_c(\theta)$  are the length, the moment of inertia, and the tangent stiffness of the connection element, respectively. When the element is loading,  $K_c(\theta)$  is evaluated using Eq. (1) as:

$$K_c(\theta) = \frac{dM}{d\theta} = \frac{(k - k_p)}{\left(1 + \left|\frac{(k - k_p)\theta}{M_0}\right|^N\right)^{\frac{N+1}{N}}} + k_p \quad (11)$$

When the element is unloading and reloading,  $K_c(\theta)$  can be calculated using Eq. (2) as:

$$K_c(\theta) = \frac{dM}{d\theta} = \frac{(k - k_p)}{\left(1 + \left| \frac{(k - k_p)(\theta_a - \theta)}{2M_0} \right|^N\right)^{\frac{N+1}{N}}} + k_p \quad (12)$$

The basic FEM formulation of the structure remains unchanged, except for adding a few more elements to represent PR connections.

### 3.1.2. Incorporation of RC shear walls into the FEM

Once the explicit form of the stiffness matrix of shear walls is obtained by using Eq. (3), it can be combined with the stiffness of the steel frame to develop stiffness matrix for the combined system. In general, the nonlinear governing equation for the combined system can be represented in the incremental form as:

$$\mathbf{K}_T^{(n)} \Delta \mathbf{D}^{(n)} = \mathbf{F}^{(n)} - \left[ \mathbf{R}^{(n-1)} + \mathbf{K}_{sh}^{(n-1)} \mathbf{D}^{(n-1)} \right] \quad (13)$$

where  $\mathbf{K}_T^{(n)} = \mathbf{K}^{(n)} + \mathbf{K}_{sh}^{(n)}$ ,  $\mathbf{K}_{sh}^{(n)}$  is the global tangent stiffness matrix of the shear walls at the  $n^{\text{th}}$  iteration,  $\mathbf{K}_{sh}^{(n-1)} \mathbf{D}^{(n-1)}$  is the internal force vector of the shear walls at the  $(n-1)^{\text{th}}$  iteration, and  $\mathbf{K}^{(n)}$ ,  $\Delta \mathbf{D}^{(n)}$ ,  $\mathbf{F}^{(n)}$ , and  $\mathbf{R}^{(n-1)}$  are defined earlier. Using Eq. (8), the equilibrium equation of the combined system can be expressed as:

$$\mathbf{M}^{t+\Delta t} \ddot{\mathbf{D}}^{(n)} + \mathbf{C}^{t+\Delta t} \dot{\mathbf{D}}^{(n)} + \mathbf{K}_T^{(n)} \mathbf{D}^{(n)} = \mathbf{F}^{(n)} - \left[ \mathbf{R}^{(n-1)} + \mathbf{K}_{sh}^{(n-1)} \mathbf{D}^{(n-1)} \right] - \mathbf{M}^{t+\Delta t} \ddot{\mathbf{D}}_g^{(n)} \quad (14)$$

Equation (14) is solved using the modified Newton-Raphson method with the arc-length procedure. The deterministic formulation of the problem discussed above is expected to be very accurate and efficient. The finite element representation of the RC shear walls is kept simple in order to minimize the number of basic random variables

present in the formulation. More sophisticated methods can be attempted in future studies, if desired. Reliability evaluation procedures are emphasized in this study.

### 3.2 Systematic response surface method

The limit state functions for the combined system discussed earlier are expected to be implicit. The RSM can be used to approximately generate the limit state or performance functions (Bucher & Bourgund, 1990 Rajashekhar & Ellingwood, 1993). At least a second order polynomial is necessary for the nonlinear dynamic problem under consideration. The following two types of second order polynomial are considered:

$$\hat{g}(\mathbf{X}) = b_0 + \sum_{i=1}^k b_i X_i + \sum_{i=1}^k b_{ii} X_i^2 \quad (15)$$

$$\hat{g}(\mathbf{X}) = b_0 + \sum_{i=1}^k b_i X_i + \sum_{i=1}^k b_{ii} X_i^2 + \sum_{i=1}^{k-1} \sum_{j>i}^k b_{ij} X_i X_j \quad (16)$$

where  $X_i$  ( $i = 1, 2, \dots, k$ ) is the  $i^{\text{th}}$  random variable, and  $b_0$ ,  $b_i$ ,  $b_{ii}$ , and  $b_{ij}$  are coefficients of the second order polynomial. The polynomial can be fully defined from regression analysis or by solving a set of simultaneous equations using information on responses obtained at specific data points called sampling points. The selection of sampling points is a crucial factor in establishing the efficiency and accuracy of RSM. Saturated design (SD) and central composite design (CCD) are the two most promising techniques used for this purpose. By considering the two design methods and the form of the polynomial, the three promising response surface models suggested by Huh and Haldar (2001) are: Model (1) - SD using a second order polynomial without cross terms, Model (2) - SD using a full second order polynomial, and Model (3) - CCD using a full second order polynomial. They are discussed in more detail elsewhere (Huh, 2000 Huh and Haldar, 2001 Huh and Haldar, 2002).

Since the proposed algorithm is iterative, it is

necessary to improve on the selection of the location of the center point around which the sampling points are generated in subsequent iterations. Bucher and Bourgund (1990) suggested an iterative linear interpolation scheme as shown in Fig. 2 and it is used in this study. It can be mathematically represented as:

$$\mathbf{x}_{C_2} = \mathbf{x}_{C_1} + (\mathbf{x}_{D_1} - \mathbf{x}_{C_1}) \frac{g(\mathbf{x}_{C_1})}{g(\mathbf{x}_{C_1}) - g(\mathbf{x}_{D_1})} \quad \text{if } g(\mathbf{x}_{D_1}) \geq g(\mathbf{x}_{C_1}) \quad (17)$$

$$\mathbf{x}_{C_2} = \mathbf{x}_{D_1} + (\mathbf{x}_{C_1} - \mathbf{x}_{D_1}) \frac{g(\mathbf{x}_{D_1})}{g(\mathbf{x}_{D_1}) - g(\mathbf{x}_{C_1})} \quad \text{if } g(\mathbf{x}_{D_1}) < g(\mathbf{x}_{C_1}) \quad (18)$$

where  $\mathbf{x}_{C_1}$  and  $\mathbf{x}_{D_1}$  are the coordinates of the center point and the checking point for the first iteration, and  $g(\mathbf{x}_{C_1})$  and  $g(\mathbf{x}_{D_1})$  are the actual responses of the limit state function estimated from dynamic FEM analysis at  $\mathbf{x}_{C_1}$  and  $\mathbf{x}_{D_1}$ , respectively. The point  $\mathbf{x}_{C_2}$  can be used as a new center point for the next iteration. This iteration scheme needs to be continued until a preselected convergence criterion is satisfied (e.g.  $(\mathbf{x}_{C_{i+1}} - \mathbf{x}_{C_i}) / \mathbf{x}_{C_i} \leq |0.05|$  in the numer-

ical examples of this study).

The proposed reliability evaluation scheme is iterative in nature. Thus, the efficiency of the scheme can be improved further during the iterations. Considering the three models identified earlier, Huh and Haldar (2001) suggested two promising schemes to improve computational efficiency without compromising accuracy. They are: Scheme 1 - SD using a second order polynomial without cross terms for the intermediate iterations and SD using a full second order polynomial for the final iteration, and Scheme 2 - SD using a second order polynomial without cross terms for the intermediate iterations and CCD using a full second order polynomial for the final iteration. Both schemes are considered here.

### 3.3 Consideration of uncertainty

In the deterministic formulation discussed so far, uncertainties associated with the load and resistance-related parameters need to be identified and incorporated. For steel frames considered in this

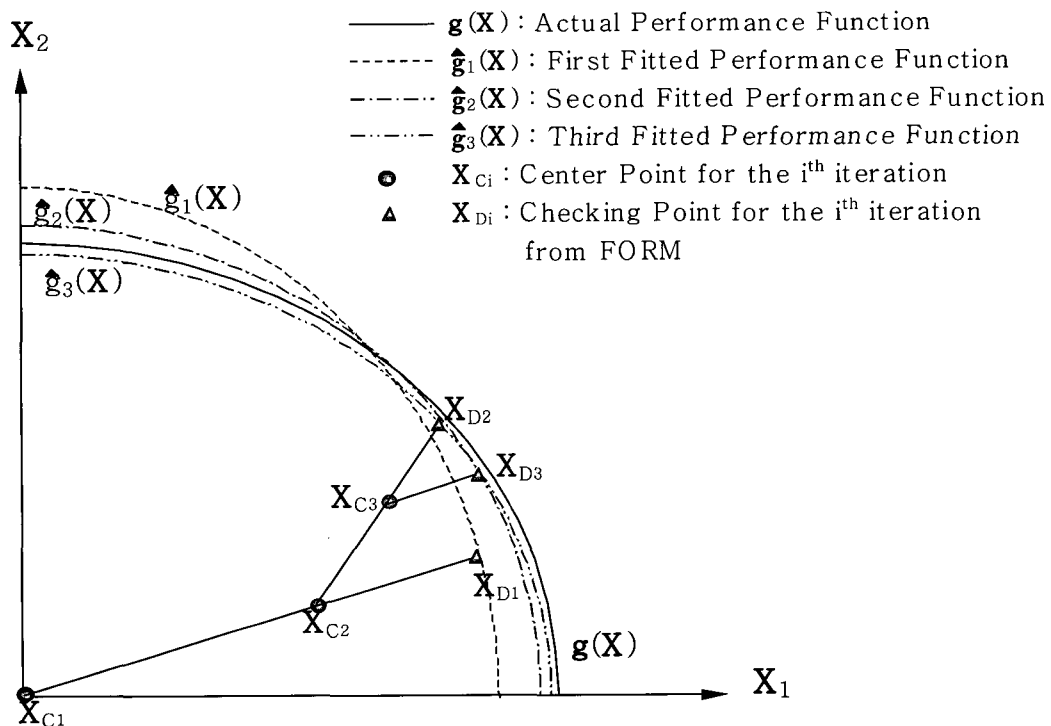


Figure 2 Iterative Linear Interpolation Scheme (Similar to Rajashekhar and Ellingwood, 1993)

paper, the resistance-related random variables are the Young's modulus ( $E$ ), the yield stress ( $F_y$ ), the cross sectional area ( $A$ ), the moment of inertia ( $I$ ), and the plastic section modulus ( $Z$ ). For the concrete shear walls, the Young's modulus ( $E_c$ ) and the Poisson's ratio ( $\nu$ ) of concrete are also considered to be random variables. The probabilistic characteristics of these variables are widely available in the literature (Haldar & Mahadevan, 2000).

The uncertainties in connection behavior come from the manufacturing and assembling processes of structural elements and also from modeling uncertainties. To consider uncertainty in modeling the behavior of PR connections, the four parameters in the Richard model are considered to be the basic random variables as shown in Fig. 3.

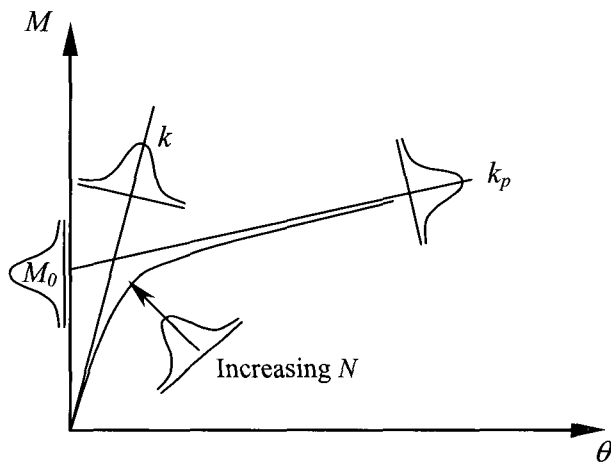


Figure 3 Random parameters in Richard model

Uncertainty in the seismic loading applied in time domain needs to be considered at this stage. However, no guideline is available on how to consider the uncertainties in both the amplitude and frequency content of the seismic loading. The uncertainty in the amplitude of the earthquake is considered in this study by treating it as a random variable. It is conceptually shown in Fig. 4. A parameter  $g_e$  is introduced to incorporate the uncertainty in the amplitude. The uncertainty in the frequency content of an earthquake is considered indirectly. The large number of time histories recorded in close proximity of each other during a

specific earthquake can be used for this purpose. They have different frequency content and the estimated reliability of a given structure will indicate the effect of uncertainty in the frequency content. The uncertainty in the frequency content can also be simulated but it is beyond the scope of this paper.

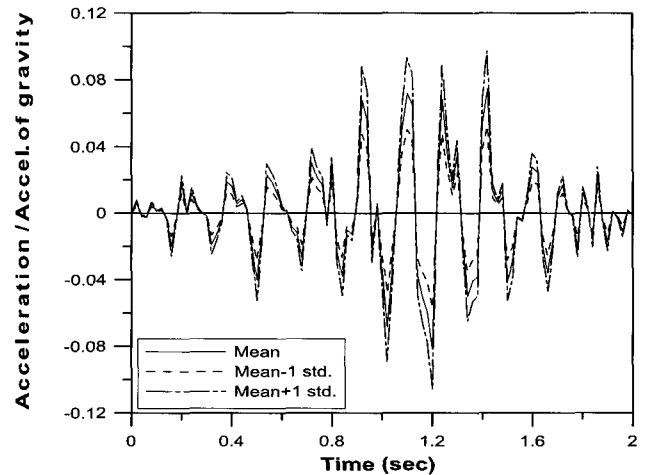


Figure 4 Consideration of uncertainty in the amplitude of an earthquake

### 3.4 Limit state functions

Risk is always estimated corresponding to a performance or limit state function. Commonly used limit state functions can be broadly divided into two groups: the serviceability and strength limit states. Each limit state needs to be considered separately since a structure can fail due to excessive lateral or inter-story deflection, or due to failure of several components in strength forming a local or global mechanism. The proposed algorithm is capable of calculating risk for both types of limit states, as discussed next.

#### 3.4.1 Strength limit state

The limit state function for structural strength mainly depends on the failure mode to be considered. Most of the elements in the structural system considered in this study are beam-columns, i.e., they are subjected to both axial load and bending moment at the same time. For design pur-



poses, interaction equations are generally used to consider the combined effect of axial load and bending moment. Thus, the interaction equations suggested by the American Institute of Steel Construction's (AISC's) *Load and Resistance Factor Design (LRFD)* manual (AISC, 1994) for two dimensional structures are used. They are:

$$\frac{P_u}{\phi P_n} + \frac{8}{9} \left( \frac{M_{ux}}{\phi_b M_{nx}} \right) \leq 1.0 \quad \text{if} \quad \frac{P_u}{\phi P_n} \geq 0.2 \quad (19)$$

$$\frac{P_u}{2\phi P_n} + \left( \frac{M_{ux}}{\phi_b M_{nx}} \right) \leq 1.0 \quad \text{if} \quad \frac{P_u}{\phi P_n} < 0.2 \quad (20)$$

where  $\phi$  and  $\phi_b$  are the resistance factors,  $P_u$  is the required tensile or compressive strength,  $P_n$  is the nominal tensile/compressive strength,  $M_{ux}$  is the required flexural strength and  $M_{nx}$  is the nominal flexural strength.  $P_n$  and  $M_{nx}$  can be calculated using the AISC's LRFD code.

### 3.4.2 Serviceability limit state

For seismic loading, the design may be controlled by the serviceability, e.g., inter-story drift or the overall lateral displacement. Limit states corresponding to inter-story drift or overall lateral displacement can be formulated using the recommendations given in design codes. The general form of a serviceability limit state can be represented as:

$$g(\mathbf{X}) = \delta_{allow} - y_{max}(\mathbf{X}) \quad (21)$$

where  $\delta_{allow}$  is the allowable inter-story drift or overall lateral displacement specified in codes and  $y_{max}(\mathbf{X})$  is the corresponding maximum inter-story drift or overall lateral displacement estimated from the analysis.

### 3.5 Solution strategy for the algorithm

The solution strategy for the proposed algorithm can be stated as follows. The initial center point is first assumed to be mean values of the random

variables for the first iteration for both schemes. Responses are calculated by conducting nonlinear FEM at the experimental sampling points for the response surface model being considered. A limit state function is thus generated in terms of  $k$  basic random variables. Using the explicit expression for the limit state function and the FORM, the reliability index  $\beta$  and the corresponding coordinates of the checking point and direction cosines for each random variable are obtained. The coordinates of the new center point are obtained by applying the linear interpolation scheme. The updating of the location of the center point continues until it converges to a predetermined tolerance level. In the final iteration, the information on the most recent center point is used to formulate the final response surface using either Scheme 1 or Scheme 2. The FORM is then used to calculate the reliability index and the corresponding coordinates of the most probable failure point.

## 4. NUMERICAL EXAMPLE

Following three examples are provided to elaborate the algorithm presented in this study and to investigate the effect of PR connection conditions and the presence of RC shear walls on the overall reliability of steel frames subjected to seismic loading. The first example considers a two-story one-bay steel frame and its connections are first considered to be FR type, a common assumption in analyzing such a frame. Connections are then considered to be PR type in the second example. In the final example, the reliability of the same steel frame with the presence of RC shear walls is evaluated. The corresponding reliabilities of the frame in the presence of FR and PR type connections, and with shear walls are evaluated using the method discussed here and compared.

### 4.1 Steel frame structure with FR connections

A two-story frame structure that consists of W24×68 for all beams and W14×257 for all columns

is considered as shown in Fig. 5. They are made of A36 steel. The self weights of beams and columns plus additional dead loads of 14.6kN/m and 7.30kN/m, respectively, are considered in estimating the mass of beam and column elements.

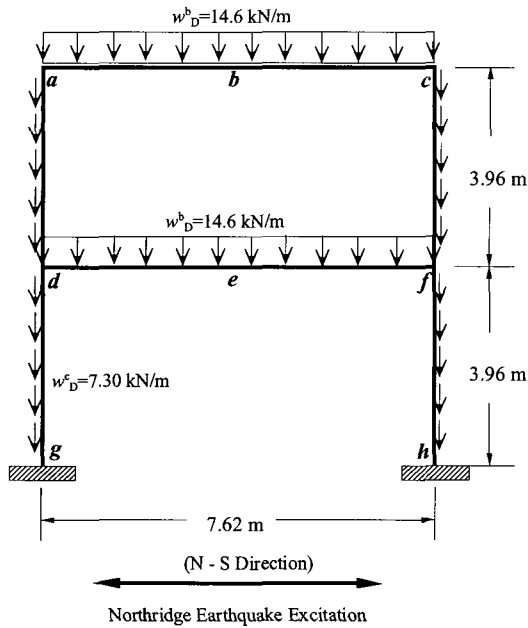


Figure 5 Two-story steel frame structure

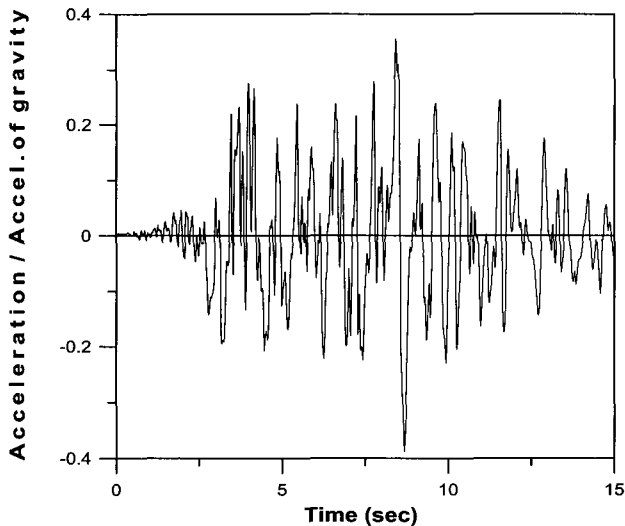


Figure 6 Northridge earthquake (N-S) time history

The frame is excited for 15 seconds by the actual acceleration time history recorded at Canoga Park during the Northridge earthquake of 1994 (N-S component) as shown in Fig. 6. Both the serviceability and strength limit states are considered. For the serviceability limit state, the permissible lateral

displacement at the top of the frame is assumed not to exceed  $h/400$ , where  $h$  is the height of the frame. Thus,  $\delta_{allow}$  is 1.98cm for this example and the corresponding limit state is:

$$g(\mathbf{X}) = \delta_{allow} - y_{max}(\mathbf{X}) = 1.98 - y_{max}(\mathbf{X}) \quad (22)$$

where  $y_{max}(\mathbf{X})$  is the maximum lateral displacement at the top of the frame. For the strength limit state, the reliabilities of the weakest beam and column members (beam  $e-f$  and column  $f-h$  in Fig. 5) are investigated.

All nine variables shown in Table 1 are considered to be random for both the serviceability and strength limit states in the initial sensitivity analysis. From the sensitivity analysis, the plastic section modulus of the beams and the yield stress of the frame ( $Z_x^b$  and  $F_y$ ) for the serviceability limit state, and the sectional area of the beams and columns ( $A^b$  and  $A^c$ ) for the strength limit state were found to have very low sensitivity indexes. They are considered to be deterministic in the subsequent reliability analyses.

Table 1 Statistical description of random variables (b: beam, c: column)

Random Variables	Mean Value	Serviceability Limit State		Strength Limit State			
				Beam (e-f)		Column (f-h)	
		COV	Dist.	COV	Dist.	COV	Dist.
E (kN/m <sup>2</sup> )	$1.999 \times 10^3$	0.06	LN	0.06	LN	0.06	LN
A <sup>b</sup> (m <sup>2</sup> )	$1.297 \times 10^{-2}$	0.05	LN	-	-	-	-
I <sub>x</sub> <sup>b</sup> (m <sup>4</sup> )	$7.617 \times 10^{-4}$	0.05	LN	0.05	LN	0.05	LN
Z <sub>x</sub> <sup>b</sup> (m <sup>3</sup> )	$2.901 \times 10^{-3}$	-	-	0.05	LN	-	-
A <sup>c</sup> (m <sup>2</sup> )	$4.877 \times 10^{-2}$	0.05	LN	-	-	-	-
I <sub>x</sub> <sup>c</sup> (m <sup>4</sup> )	$1.415 \times 10^{-3}$	0.05	LN	0.05	LN	0.05	LN
Z <sub>x</sub> <sup>c</sup> (m <sup>3</sup> )	$2.901 \times 10^{-3}$	-	-	-	-	0.05	LN
F <sub>y</sub> (kN/m <sup>2</sup> )	$2.482 \times 10^5$	-	-	0.10	LN	0.10	LN
ξ	0.05	0.15	LN	0.15	LN	0.15	LN
g <sub>e</sub>	1.00	0.20	Type I	0.20	Type I	0.20	Type I

The frame is analyzed assuming the connections are FR type. The statistical characteristics of all the random variables for both limit states are also given in Table 1. The term  $\xi$  in Table 1 represents the viscous damping coefficient expressed as a per-

cent of the critical damping. The probabilities of failure of the frame are estimated using Scheme 2 in this example to increase the accuracy of the results. The results for both limit states are tabulated in Table 2 in terms of failure probability, reliability index, error, number of random variables considered and total number of experimental sampling points (TNSP). For the verification purpose the results are compared with Monte Carlo simulation (MCS) using 50,000 simulations. The error estimation for the serviceability limit state is based on the failure probability. The reliability index is used to estimate the error for the strength limit state since the failure probability is too small to compare. An IBM personal computer was used for the numerical calculation for the proposed algorithm and MCS.

Table 2 Reliability analysis results of the frame with FR connections

Limit State		Serviceability	Strength	
			Beam (e-f)	Column (f-h)
MCS	$P_f$	0.17786	0.00008	0.00000
	$\beta \approx \Phi^{-1}(1-P_f)$	0.924	3.775	N/A
	NOS	50,000	50,000	50,000
Proposed Method	Scheme	Scheme 2	Scheme 2	Scheme 2
	No. of R.V.	7	7	7
	$\beta$	0.873	3.736	4.361
	$P_f \approx \Phi^{-1}(-\beta)$	0.17952	0.000012	$6.48 \times 10^{-6}$
	TNSP	173	173	173
Error	-0.9 %	1.0 %	N/A	

Results in Table 2 clearly indicate that the probabilities of failure estimated using the proposed algorithm for both limit states are very similar to MCS, however, the ratio of total number of FEM analyses for MCS to that of the proposed algorithm is approximately 290. The results clearly indicate that instead of using 50,000 simulations, few hundreds carefully selected simulations can be conducted using the proposed algorithm without compromising any accuracy. Thus, the proposed method is viable and efficient for the reliability of non-linear frame structures subjected to dynamic loading including seismic loading applied in time domain.

#### 4.2 Steel frame structures with PR connections

The four beam-to-column connections at a, c, d, and f of the same frame shown in Fig. 5 are considered to be partially restrained. Three  $M-\theta$  curves, Curve 1, Curve 2, and Curve 3, are shown in Fig. 7. Curve 1 represents high rigidity, Curve 3 represents very low rigidity, and Curve 2 represents intermediate rigidity.

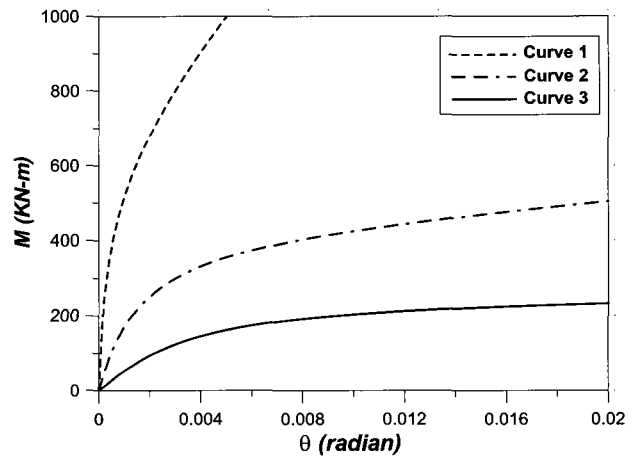


Figure 7  $M-\theta$  curves for connections

The probabilistic descriptions of the four parameters of the Richard model representing the three curves are listed in Table 3. The statistical descriptions of all other random variables remain the same as in Table 1. As in the previous example, the frame is excited by the same acceleration time history recorded at Canoga Park during the Northridge earthquake of 1994. The same serviceability and strength limit states are considered in this example.

Table 3 Statistical description of the four parameters in the Richard model

Random Variables	Mean Value			COV	Distribution
	Curve 1	Curve 2	Curve 3		
$k$ (kN·m/rad)	$1.00 \times 10^7$	$2.51 \times 10^5$	$5.65 \times 10^4$	0.15	Normal
$k_p$ (kN·m/rad)	$6.89 \times 10^3$	$5.56 \times 10^3$	$9.04 \times 10^2$	0.15	Normal
$M_0$ (kN·m)	$9.64 \times 10^2$	$4.16 \times 10^2$	$2.26 \times 10^2$	0.15	Normal
$N$	0.50	1.1	1.5	0.05	Normal

The probabilities of failure of the frame are estimated using the proposed method using Scheme 1 for PR connections with 11 random variables. The results for both limit states of the frame with PR connections represented by Curve 2 are tabulated in Table 4. For the verification purpose the results are again compared with Monte Carlo simulation (MCS) results using 50,000 simulations. Results in Table 4 indicate that the probabilities of failure estimated using the proposed algorithm in both limit states are also very similar to MCS, however, the ratio of total number of FEM analyses for MCS to that of the proposed algorithm is approximately 403. The results clearly indicate that for the frame with PR connections, the proposed method provides an additional efficiency. Thus, the proposed method is viable and efficient for the reliability of non-linear frame structures in the presence of PR connections subjected to seismic loading applied in time domain.

Table 4 Reliability analysis results of the frame with PR connections represented by Curve 2

Limit State		Serviceability	Strength	
			Beam (e-f)	Column (f-h)
MCS	$P_f$	0.39892	0.00248	0.00198
	$\beta \approx \Phi^{-1}(1-P_f)$	0.256	2.810	2.881
	NOS	50,000	50,000	50,000
Proposed Method	Scheme No. of R.V.	Scheme 1 11	Scheme 1 11	Scheme 1 11
	$\beta$	0.292	2.920	3.062
	$P_f \approx \Phi^{-1}(\beta)$	0.38514	0.00175	0.00110
	TNSP	124	124	124
	Error	3.5 %	-3.9 %	-6.3 %

Table 5 Reliability indexes of a steel frame with either FR or PR connections

Limit State	FR Conn.	PR Connections		
		Curve 1	Curve 2	Curve 3
Serviceability	$\beta = 0.873$	$\beta = 0.620$	$\beta = 0.292$	$\beta = -1.412$
Strength	Beam	$\beta = 3.736$	$\beta = 2.288$	$\beta = 4.013$
	Column	$\beta = 4.361$	$\beta = 2.322$	$\beta = 4.108$

The reliability indexes of the frame with FR and three different PR connections are summarized in

Table 5. From the results in Table 5, it can be observed that the reliability indexes for the serviceability limit state decreased significantly with the decrease in the rigidity of the PR connections. This behavior is expected. The frame became very weak in serviceability, particularly when PR connections were represented by very flexible Curve 3. Due to the redistribution of moment in beam e-f, the reliability indexes for the strength limit state also changed. However, the frame found to be more prone to failure in serviceability than in strength. It can be concluded that connection rigidity should be taken into account appropriately in reliability analysis of steel frame structures subjected to seismic loading.

### 4.3 Reliability analysis of In-filled steel frame structures

The frame without shear walls is found not to be able to carry the seismic load applied to it. The frame reinforced with RC shear walls is shown in Fig. 8. As discussed before, two additional random variables related to the shear walls,  $E_c$  and  $\nu$ , need to be considered. Their statistical properties are given in Table 6. The statistical characteristics of other random variables remain the same as in the previous cases.

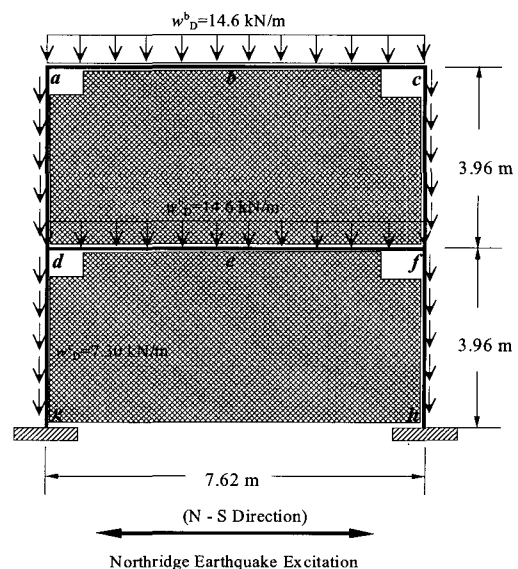


Figure 8 A frame structure with shear walls

Table 6 Statistical description of random variables

Item	Random Variables	Mean Value	COV	Dist.	Comment
Shear Wall	$E_c$ (kN/m <sup>2</sup> )	$2.140 \times 10^7$	0.18	LN	$f'_c = 2.068 \times 10^4$ (kN/m <sup>2</sup> )
	$\nu$	0.17	0.10	LN	

Table 7 Reliability Analysis Result in consideration of shear walls

Item	Connection Type	
	FR	PR
Without Shear Walls	$\beta = 0.873$	$\beta = 0.292$
With Shear Walls	$\beta = 3.615$	$\beta = 3.246$

Although the physical thickness of the shear wall is considered to be 12.7cm, considering the presence of frames and rigid behavior of diaphragms, the effective thickness per frame is assumed to be 2.54cm for this example. After the tensile stress of each shear wall exceeds the prescribed tensile stress of concrete, the degradation of the shear wall stiffness is assumed to be reduced to 40% of the original stiffness (Lefas et al., 1990).

The frame is again excited for 15 seconds by the same Northridge earthquake of 1994 (N-S component) as shown in Fig. 6. The probabilities of failure for the combined system in presence of FR connections and PR connections using Curve 2 for the serviceability limit state are calculated using the proposed algorithm with Scheme 1. The horizontal deflection at the top of the combined system (point *c* in Fig. 8) is evaluated. The results are summarized in Table 7. The results indicate that the presence of shear walls significantly improves the serviceability behavior of the steel frame. This behavior is expected. However, the amount of improvement in terms of probability of failure can be quantified using the proposed algorithm considering major sources of uncertainty.

Three realistic examples clearly demonstrate the power of the proposed algorithm. The proposed algorithm is expected to be very useful in the performance-based design guidelines under development by the profession. It will help to develop risk-consistent design requirements. Assuming the reliability of a structure should be similar for both

the serviceability and strength limit states, the algorithm will help to develop the allowable deflection criterion. For example, the current allowable lateral deflection criterion of  $h/400$  may be too conservative.

### 5. CONCLUSIONS

A stochastic finite element-based algorithm is proposed to evaluate the reliability of real structures subjected to seismic loading applied in time domain, considering all major sources of non-linearity and uncertainty. The unique feature of the technique is that the seismic loading is applied in the time domain, providing an alternative to the classical random vibration approach. The procedure rationally and effectively combines the concepts of the RSM, the FEM, the FORM, and the iterative linear interpolation scheme.

The four-parameter Richard model is used to represent the flexibility of connections of real steel frames. Uncertainties in the loading and resistance-related parameters and the parameters in the Richard model are incorporated in the algorithm. The algorithm was elaborated by evaluating the probabilities of failure of steel frames with FR and PR connections. The flexibility of connections and the uncertainty in modeling them have a considerable amount of influence on the overall behavior of frames, particularly under seismic loading. The applicability of the methods to estimate the reliability of real structures is extended in the last example by considering a steel frame reinforced with RC shear walls. The algorithm is shown to be accurate and efficient. It is capable of estimating the reliability of any real structure that can be represented by finite elements.

This is a very advanced form of reliability analysis technique for seismic loading applied in time domain explicitly considering the uncertainty associated it. The procedure appears to be very useful in the performance-based design guidelines under development by the profession. In other words, the

member sizes and arrangements based on the performance requirements can be established with the help of the proposed algorithm. In the analysis and design of structures, uncertainty in seismic loading should not be overlooked.

### Acknowledgments

This work was supported by the Korea Research Foundation Grant(KRF-2003-003-D00447).

### References

- American Institute of Steel Construction (1994) *Manual of Steel Construction: Load and Resistance Factor Design*, Chicago, Illinois.
- Bucher, C.G., Bourgund, U. (1990) A fast and efficient response surface approach for structural reliability problems. *Structural Safety*, 7, pp.57~66.
- Colson, A. (1991) Theoretical modeling of semirigid connections behavior. *Journal of the Construction steel Research*, 19, pp.213~224
- Clough, R. W., Penzien, J. (1993) *Dynamics of Structures 2<sup>nd</sup> Edition*, McGraw-Hill, New York, N.Y.
- El-Salti, M. K. (1992) *Design of frames with partially restrained connections*, Ph.D. Dissertation, Dept. Of Civil Engineering and Engineering Mechanics, The University of Arizona, Tucson, Arizona, U.S.A.
- Gupta, A.K., Akbar, H. (1983) Cracking in reinforced concrete analysis. *Journal of Structural Engineering*, ASCE, 107 (ST1), pp.1735~1746.
- Haldar, A., Gao, L. (1997) Reliability evaluation of structures using nonlinear SFEM. *Uncertainty Modeling in Finite Element, Fatigue, and Stability of Systems*, A. Haldar, A. Guran, and B.M. Ayyub, eds., World Scientific Publishing Co., River Edge, N.J., pp.23~50.
- Haldar, A., Mahadevan, S. (2000) *Probability, Reliability And Statistical Methods In Engineering Design*. John Wiley & Sons, New York, N.Y.
- Haldar, A., Nee, K. M. (1989) Elasto-Plastic Large Deformation Analysis of PR Steel Frames for LRFD. *Computers and Structures*, 31(5), pp.811~823.
- Huh, J. (2000) Nonlinear Structural Safety Assessment under Dynamic Excitation Using SFEM. *Journal of the Computational Structural Engineering Institute of Korea*, 13(3), pp.373~384.
- Huh, J., Haldar, A. (2001) Stochastic Finite-Element-Based Seismic Risk of Nonlinear Structures. *Journal of Structural Engineering*, ASCE, 127( 3), pp.323~329.
- Huh, J., Haldar, A. (2002) Seismic reliability of non-linear frames with PR connections using systematic RSM. *Probabilistic Engineering Mechanics*, 17, pp.177~190.
- Huh, J., Cho, H-N. (2001) Effect of Partially Restrained Connections on Seismic risk Evaluation of Steel Frames. *Journal of the Computational Structural Engineering Institute of Korea*, 14(4), pp.537~549.
- Inoue, N., Yang, K., Shibata, A. (1997) Dynamic nonlinear analysis of reinforced concrete shear wall by finite element method with explicit analytical procedure. *Earthquake Engineering and Structural Dynamics*, 26, pp.967~986.
- Kondoh, K., Atluri, S. N. (1987) Large-deformation, elasto-plastic analysis of frames under nonconservative loading, using explicitly derived tangent stiffnesses based on assumed stresses. *Computational Mechanics*, 2(1), pp.1~25.
- Lee, S.Y. (2000) *Static and dynamic reliability analysis of frame and shear wall structural systems*. Ph.D. Dissertation, Dept. of Civil Engineering and Engineering Mechanics, The University of Arizona, Tucson, Arizona, U.S.A.
- Lefas, D., Kotsovos, D. & Ambraseys, N. (1990) Behavior of reinforced concrete structural walls: strength, deformation characteristics, and failure mechanism. *ACI Structural Journal*, 87(1), pp.23~31
- Leger, P., Dussault, S. (1992) Seismic energy dissipation in MDOF structures, *Journal of Structural Engineering*, ASCE, 118(5), pp.1251~1269.
- Liauw, T.C., Kwan, K.H. (1985) Static and cyclic behaviors of multistory infilled frames with different interface conditions. *Journal of Sound and Vibration*, 99(2), pp.275~283.
- Rajashekhhar, M.R., Ellingwood, B. R. (1993)

A new look at the response surface approach for reliability analysis. *Structural Safety*, 12, pp.205~220.

**Richard, R. M., Abbott, B.J.** (1975) Versatile elastic-plastic stress-strain formula. *Journal of Engineering Mechanics, ASCE*, 101(EM4), pp.511~515.

**Shi, G., Atluri, S. N.** (1988) Elasto-plastic large deformation analysis of space frames. *Int. J. for Num. Methods in Eng.*, 26, pp.589~615.

**Vecchio, F.J.** (1989) Nonlinear finite element analysis of reinforced concrete membranes. *ACI Structural Journal*, 86(1), pp.26~35.